

Schwarzschild black holes can wear scalar wigs

Juan Barranco,¹ Argelia Bernal,² Juan Carlos Degollado,³ Alberto Diez-Tejedor,¹
Miguel Megevand,² Miguel Alcubierre,² Darío Núñez,² and Olivier Sarbach⁴

¹*Departamento de Física, División de Ciencias e Ingeniería,
Campus León, Universidad de Guanajuato, León 37150, México*

²*Instituto de Ciencias Nucleares, Universidad Nacional Autónoma de México,
Circuito Exterior C.U., A.P. 70-543, México D.F. 04510, México*

³*Instituto de Astronomía, Universidad Nacional Autónoma de México,
Circuito Exterior C.U., A.P. 70-264, México D.F. 04510, México*

⁴*Instituto de Física y Matemáticas, Universidad Michoacana de San Nicolás de Hidalgo,
Edificio C-3, Ciudad Universitaria, 58040 Morelia, Michoacán, México*

(Dated: December 29, 2017)

We study the evolution of a massive scalar field surrounding a Schwarzschild black hole and find configurations that can survive for arbitrarily long times, provided the black hole or the scalar field mass is small enough. In particular, both ultra-light scalar field dark matter around supermassive black holes and axion-like scalar fields around primordial black holes can survive for cosmological times. Moreover, these results are quite generic, in the sense that fairly arbitrary initial data evolves, at late times, as a combination of those long-lived configurations.

PACS numbers: 95.30.Sf, 98.62.Mw, 95.35.+d, 98.62.Gq

I- Introduction. It has been known for some time that a Schwarzschild black hole (BH) cannot support a nontrivial scalar field (SF) distribution, i.e. such a hole does not admit scalar hair [1, 2]. However, the no-hair theorems do not exclude the existence of dynamical solutions that decay very slowly in time. In a recent work [3] we found regular SF configurations surrounding a Schwarzschild BH that can survive for relatively long times, and conjectured that, for a certain range of values of the SF and BH masses, such SF configurations could survive in the vicinity of the BH for cosmological timescales. Here we show that this is indeed what happens, and that such distributions arise from the evolution of fairly arbitrary initial configurations. Our results give support to the idea that the dark matter halos could be described by a coherent scalar excitation [4, 5] (see [6, 7] for papers with a similar motivation), and to the possibility of nontrivial axion distributions surrounding primordial BHs [8].

II- Three types of resonances. The dynamics of a SF propagating on a Schwarzschild background are described by the Klein-Gordon equation

$$\frac{\partial^2 \phi}{\partial t^2} - \frac{\partial^2 \phi}{\partial r_*^2} + V(r)\phi = 0, \quad (1a)$$

with $V(r)$ an effective potential given by

$$V(r) = \left(1 - \frac{2M}{r}\right) \left(\frac{\ell(\ell+1)}{r^2} + \frac{2M}{r^3} + \mu^2\right). \quad (1b)$$

Here M is the BH mass, ℓ the angular momentum number (we decompose the field in spherical harmonics), μ the mass of the SF (in units for which $G = c = \hbar = 1$), and r_* ($-\infty < r_* < +\infty$) the radial “tortoise” coordinate, related to the Schwarzschild radial coordinate r ($r > 2M$) by $r_* = r + 2M \ln(r/2M - 1)$. As discussed in detail

in [3] (see also reference [9]), for each $\ell \geq 0$ and $M\mu < M\mu_{\text{crit}}(\ell)$, V describes a potential well which is enclosed between a barrier close to the BH, and the asymptotic positive value μ^2 of the potential at infinity.

The stationary solutions of Eq. (1) are characterized by a time dependency of the form $e^{i\omega t}$ with a real frequency ω . Such solutions behave as a combination of ingoing and outgoing waves to the left of the potential barrier, close to the horizon, and we require them to decay exponentially to zero at spatial infinity. There is a continuous spectrum of such solutions for $\omega^2 < \mu^2$. Furthermore, as we have shown in [3], for ω lying in the region $V_{\text{min}} < \omega^2 < \mu^2$, with V_{min} the local minimum of the potential, there is a discrete set of such frequencies for which the amplitude inside the potential well takes very large values when compared with the amplitude close to the horizon. We call these modes the *stationary resonances*, and the region $V_{\text{min}} < \omega^2 < \mu^2$ the *resonance band*.

If one imposes the condition of no waves coming from the region close to the horizon, while keeping the requirement of exponential decay at spatial infinity, it turns out that Eq. (1) is only satisfied for a discrete set of complex frequencies. These solutions have been called *quasi-resonances* in the literature [10] (see also [11] for a previous study of such solutions).

Both the stationary resonances and quasi-resonances are in fact non-physical solutions. First, as mentioned above, all purely stationary solutions, i.e. those with real ω , require waves to move outward from the horizon region to compensate for the waves that tunnel out through the barrier and move toward the horizon (as otherwise the situation would not be stationary). Imposing the condition of no waves coming out from the horizon

clearly improves the situation at the cost of introducing complex valued frequencies ω . This makes sense physically since now the solutions must decay in time as the waves tunnel out of the potential well and fall toward the BH, with this decay represented by the imaginary part of the frequency. Nevertheless, it turns out that such solutions are still non-physical, as one can show that the energy density diverges at the horizon for both types of solutions.

There is yet a third class of resonant solutions we will consider. In reference [3] we performed numerical evolutions of regular initial data that has not such divergence of the energy density at the horizon, and found damped oscillating solutions that remain surrounding the BH for long times. These solutions have frequency equal (within the numerical error) to that of the stationary resonances. We call these solutions *dynamical resonances*. We will show that the real part of the frequency of the quasi-resonant modes coincides with the frequency of oscillation of the stationary and dynamical resonances, and that the imaginary part coincides with the decay rate of the dynamical resonances. This is a nontrivial result since, after all, the dynamical solutions are in some sense “infinitely different” to both the stationary resonances and the quasi-resonances because they are regular solutions with finite energy. This is similar to the case of the quasinormal modes of BHs, which also diverge at the horizon, but nevertheless physical excitations behave as combinations of them locally at late times.

III- Toy model. In order to illustrate how the different resonant modes arise and are related to each other, we first consider a simple toy model in which the potential V in Eq. (1b) is replaced by

$$U(x) = A\delta(x) + \mu^2\Theta(x - a), \quad x := r_*, \quad (2)$$

with A and a positive constants. That is, we have a potential well enclosed between the δ -barrier and a step function where U jumps from zero to its asymptotic value μ^2 . For $M\mu \ll 1$ and $\ell \geq 1$ the minimum of the potential well of the physical potential V is located at $r_{\min} = \ell(\ell + 1)(M\mu^2)^{-1}[1 + \mathcal{O}(M\mu^2)]$, and the strength of its barrier is $\int_{-\infty}^{r_{\min}^*} V dr_* = [6\ell(\ell + 1) + 1](4M)^{-1}[1 + \mathcal{O}(M\mu^2)]$. Therefore, we require the dimensionless parameters $\lambda := 2\mu/A$ and $p := (a\mu)^{-1}$ to scale like $M\mu$ in our toy model potential U . In the analysis below we prove that for fixed $p < 1/\pi$ and small enough values of λ , the potential U gives rise to a discrete set of stationary and quasi-resonant frequencies whose real parts agree with each other.

The resonant modes for the potential U have the form

$$\phi(t, x) = e^{i\omega t} \cdot \begin{cases} \alpha e^{i\omega x} + \beta e^{-i\omega x}, & x < 0, \\ \gamma e^{i\omega x} + \delta e^{-i\omega x}, & 0 < x < a, \\ e^{-\sqrt{\mu^2 - \omega^2}x}, & x > a, \end{cases} \quad (3)$$

with ω a complex frequency. We require $\omega \notin (-\infty, -\mu] \cup [\mu, \infty)$, which guarantees that $\text{Re}\sqrt{\mu^2 - \omega^2} \neq 0$, and

therefore we can choose the sign of the square root such that its real part is positive, leading to exponential decay for $x > a$, as required. The constants α, β, γ and δ are determined by the matching conditions at $x = 0$ and $x = a$ which consist in the continuity of ϕ and its first spatial derivative ϕ' at $x = a$ and the continuity of ϕ and the jump condition $\phi'(t, 0^+) - \phi'(t, 0^-) = A\phi(t, 0)$ at $x = 0$.

For the stationary resonances ω is real and our restrictions imply $\omega \in (-\mu, \mu)$. Since U is real, it follows in this case that $\alpha = \beta^*, \gamma = \delta^*$, and the ratio between the amplitudes of the solution for $x < 0$ and the one inside the well is $\nu(\omega) = |\alpha|/|\gamma|$. The resonance frequencies are the ones that minimize this ratio. For the quasi-resonances, in turn, the condition of no waves coming from the horizon implies that $\beta = 0$, which can only occur for a non-trivial imaginary part of ω . In terms of the quantities λ and p defined below Eq. (2), and the complex angle φ lying inside the strip $-\pi/2 < \text{Re}(\varphi) < \pi/2$ defined by $\omega = \mu \sin \varphi$, the condition $\beta = 0$ reads

$$F_p(\lambda, \varphi) := 1 + i\lambda \sin \varphi - e^{-2i\varphi - \frac{2i}{p} \sin \varphi} = 0, \quad (4)$$

while the ratio of interior and exterior solutions in the stationary case is

$$\nu(\omega) = \frac{1}{\lambda} \frac{|F_p(\lambda, \varphi)|}{\sin \varphi}. \quad (5)$$

As we prove now there exists, for each $p < 1/\pi$ and small enough λ , a finite family $\varphi_n(\lambda)$ of solutions of Eq. (4) with the following properties: they depend smoothly on λ , their imaginary parts decay like λ^2 , and their real parts agree with the local minima of $\nu(\omega)$. This shows the existence of quasi-resonant modes for the toy model potential U whose frequencies are related to those of the stationary resonant modes through their real parts.

In order to show this we consider first the limit $\lambda = 0$, in which case Eq. (4) yields real solutions $\varphi_n^{(0)} \in (-\pi/2, \pi/2)$ satisfying $\sin \varphi_n^{(0)} = p(n\pi - \varphi_n^{(0)})$, with $n = 1, 2, 3, \dots$. There are a finite number of solutions when $p < 1/\pi$. For $p \ll 1/\pi$ the fundamental solution is approximately $\varphi_1^{(0)} \approx p\pi$. In order to extend these solutions for small $\lambda > 0$ we invoke the implicit function theorem and observe that the function $F_p(\lambda, \varphi)$ is linear in λ and analytic in φ . Furthermore, $\frac{\partial F_p}{\partial \varphi}(0, \varphi_n^{(0)}) = 2i(1 + p^{-1} \cos \varphi_n^{(0)}) \neq 0$ since $-\pi/2 < \varphi_n^{(0)} < \pi/2$. Therefore, there exists for small enough λ a unique smooth solution curve $\varphi_n(\lambda)$ satisfying $F_p(\lambda, \varphi_n(\lambda)) = 0$ and $\varphi_n(0) = \varphi_n^{(0)}$. A Taylor expansion reveals that the corresponding complex frequencies $\omega_n(\lambda) = \mu \sin(\varphi_n(\lambda))$ have the form

$$\text{Re}(\omega_n(\lambda)) = \mu \sin \varphi_n^{(0)} \left[1 - \frac{\lambda}{q_n} + \frac{\sigma}{q_n^2} \lambda^2 + \mathcal{O}(\lambda^3) \right], \quad (6a)$$

$$\text{Im}(\omega_n(\lambda)) = \frac{\mu \sin^2 \varphi_n^{(0)}}{2} \frac{\lambda^2}{q_n} + \mathcal{O}(\lambda^3), \quad (6b)$$

where we have defined $q_n := 2(\cos^{-1} \varphi_n^{(0)} + p^{-1})$ and $\sigma := 1 - q_n^{-1} \sin^2 \varphi_n^{(0)} / \cos^3 \varphi_n^{(0)}$. Furthermore, one can verify that the local minima of the function $\nu(\omega)$ given in Eq. (5), describing the stationary resonances, have precisely the expansion given in Eq. (6a). Therefore, up to second order in λ , the frequencies of the stationary resonances agree with the real part of the quasi-resonant frequencies.

Since both parameters λ and p scale like $M\mu$ in our model potential, it follows that for $M\mu \ll 1$ the imaginary part of $M\omega_n$ scales like $(M\mu)^6$. This explains, at least qualitatively, why the quasi-resonant modes are associated with such large time-scales when $M\mu \ll 1$.

It is also possible to relate the quasi-resonant frequencies ω_n to the dynamical resonances by representing the solutions of Eq. (1) as an inverse Laplace integral. This calculation will be presented elsewhere.

IV- Frequency comparison and characteristic times. For the physical potential, Eq. (1b), the quasi-resonant modes can be obtained semi-analytically in several ways, the most common are the continued fraction method introduced by Leaver [12], and the WKB approach [13] (see [14–17] for details). An analytic expression valid for small values of the combination $M\mu$ was obtained by Detweiler in [11]. The stationary and dynamical modes were previously considered in [3]. In this section we show that the oscillations of the dynamical resonances have frequencies equal (up to numerical error) to the real part of the frequencies of the quasi-resonant modes, while the decay rates are equal to the imaginary part of such frequencies (see Fig. 1). We also show that the imaginary part of the quasi-resonant frequencies calculated by means of Leaver’s method has the limit behaviour predicted by Detweiler. Hence, we can use Detweiler expressions to determine the decay rate of the dynamical resonances with very small values of $M\mu$, which cannot be reached with the other two methods.

Leaver’s semi-analytical approach [12] assumes a harmonic time dependence for the SF, $\phi(t, r) = \psi(r)e^{i\omega t}$, with ω the complex quasi-resonant frequency, and proposes a power series expansion for the radial function $\psi(r)$ of the form

$$\psi = \tilde{\psi} \sum_{n=0}^{\infty} a_n \left(1 - \frac{2M}{r}\right)^n, \quad (7)$$

where, following Ref. [18], we define $\tilde{\psi} := e^{-\chi r} r^{(-2M\chi + M\mu^2/\chi)} (1 - 2M/r)^{-2iM\omega}$. This guarantees that close to the horizon $\psi \sim e^{i\omega r^*}$, whereas at spatial infinity $\psi \sim e^{-\chi r^*} r^{M\mu^2/\chi}$, with $\chi = \sqrt{\mu^2 - \omega^2}$ and the sign convention for the square root was explained in the previous section. Notice however that our boundary conditions are different than those in [18].

In Fig. 1 we plot the imaginary part of the frequency of the first quasi-resonant mode (the one with the lower

value of $\text{Re}(M\omega)$) for the cases $\ell = 0, 1$ and different values of $M\mu$. We find that the real part of the frequencies obtained corresponds to the frequencies at which the SF oscillates in a dynamical scenario [3]. Furthermore, we also find that the imaginary part of the frequencies (dots in Fig. 1) corresponds to the decay rate of the field in the numerical evolutions (empty circles in Fig. 1).

In the numerical evolutions we were not able to evolve the configurations for small values of $M\mu$, both because of the propagation of the errors in the numerical approximation, and because the time required for such evolutions becomes prohibitive. Even though Leaver’s method allows us to obtain results for parameter values that could not be reached with the numerical evolutions, numerical roundoff errors make it still prohibitive to obtain accurately very small values for the imaginary part of the quasi-resonant frequencies.

In reference [11] analytic expressions for the spectrum of quasi-resonant modes were found in the limit $M\mu \ll 1$, for values of $\ell \geq 1$. For $\ell = 1$, the imaginary part of the frequency for the first quasi-resonant mode in this limit is given by $\text{Im}(M\omega) = (M\mu)^{10}/6$. Strictly speaking, the expressions given in [11] may not apply for the case with $\ell = 0$. However, if we nevertheless use them in that case we find $\text{Im}(M\omega) = 16(M\mu)^6$. We have calculated the quasi-resonant mode frequencies using Leaver’s method up to the smallest values of $M\mu$ allowed by the round-off errors, and we have found that the imaginary part of such frequencies matches the Detweiler approximations (within errors) at small values of $M\mu$ (see Fig. 1). This result allows us to conclude that, for small values of $M\mu$, the decay time of the dynamical resonances should correspond to the one predicted by Detweiler in [11].

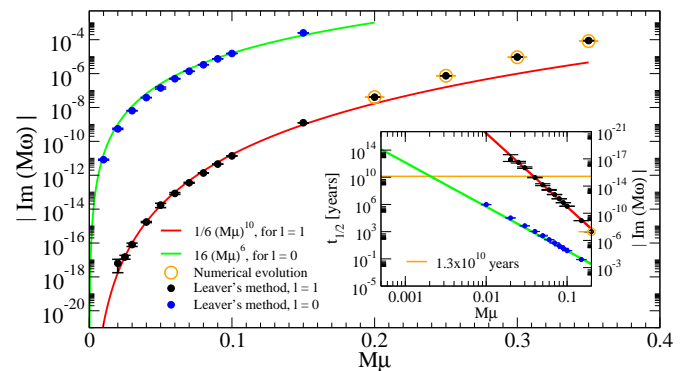


FIG. 1: The imaginary part of the frequency for the first quasi-resonant mode obtained using Leaver’s method is shown as function of $M\mu$ for the cases $\ell = 0, 1$.

Since the decay rate of the dynamical resonances is related to the imaginary part of the quasi-resonant frequencies, then its half-life time is inversely proportional to $\text{Im}(M\omega)$. In particular we can find BH and SF masses such that $t_{1/2} \sim 10^{10}$ yrs. and larger for the cases $\ell = 0, 1$ previously mentioned. Those results are shown in Fig. 2.

There are two distinct regions of the parameter space of physical interest for which the configurations live longer than the age of the Universe: (i) a SF mass smaller than 1 eV and BH mass smaller than $10^{-17}M_\odot$, consistent with primordial BHs with an axion distribution [8]; and (ii) an ultra-light (fuzzy) SF [19–21] with mass smaller than 10^{-22} eV and a supermassive BH with mass smaller than $5 \times 10^{10}M_\odot$, as could be the case for a dark matter halo [4, 5] surrounding a BH at a galactic center.

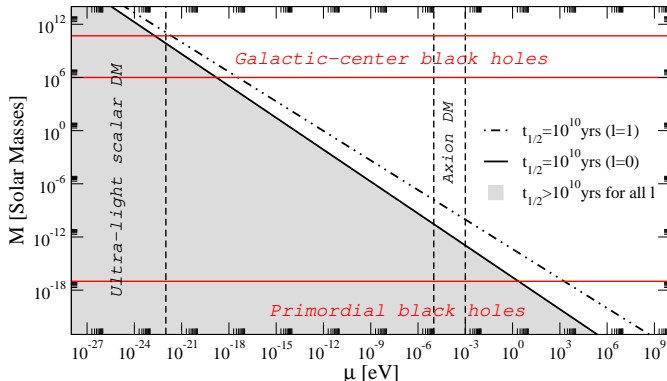


FIG. 2: Combinations of the parameters M and μ for which the SF half-life time can be larger than the age of the universe.

V- Evolution of arbitrary configurations. In this section we study the long-term numerical evolution of SF distributions that are initially surrounding a Schwarzschild BH. We show that at late times, after some SF falls into the BH and some escapes to infinity, the remaining SF consists of a superposition of the dynamical resonances, which, for practical purposes, can be described in terms of the quasi-resonant modes. Remarkably, we see that this holds even for pretty arbitrary initial data. Note that the calculations in this section are identical to those in [3], but with the crucial difference that here they are performed on arbitrary initial data (as opposed to initial data obtained from stationary resonances), hence leading to new, much stronger results.

In order to test the evolution of a variety of SF distributions, we construct a two-parameter family of initial data, of the form

$$u_0(r) = \begin{cases} N(r - R_1)^4(r - R_2)^4 & \text{for } R_1 \leq r \leq R_2 \\ 0 & \text{otherwise} \end{cases}, \quad (8)$$

with the normalization $N = [2/(R_1 - R_2)]^8$. The parameters R_1 and R_2 are chosen in order to set distributions at $t = 0$ with different “locations” and “sizes”. The initial value of the time derivative, $\dot{u}|_{t=0}$, is constructed as

$$\dot{u}|_{t=0} = \left. \frac{\partial f}{\partial t} \right|_{t=0}, \quad f(t, r) := u_0(r - vt), \quad (9)$$

where v is a free parameter that has no significant effect on the results presented here, and for the majority of con-

figurations studied is simply set to zero. The evolution equation is solved numerically, as described in [22].

As expected, during the initial stages of the evolution some SF accretes into the BH, while some is radiated away, both with rates that depend greatly on the initial data chosen, and can be very large in some cases. However, at late times, all evolutions show a similar steady behaviour with slow accretion into the BH. Similar results are obtained when studying the long-term evolution of a variety of configurations, some of them very different in size and spatial distribution –although all distributions studied here are quite “wide” when compared to the BH size.

One can gain some understanding of this behaviour by conducting a spectral analysis as follows. We perform a (discrete) Fourier transform in time, $\mathcal{F}[\phi(t, r_j)](\omega)$, of the SF at several (about 20) sample points r_j , then take the average to obtain the spectrum $\mathcal{F}[\phi(t)](\omega)$. For brevity, we present here results corresponding to only two representative examples. They correspond to initial data with $R_1 = 100M$, $R_2 = 200M$; and $R_1 = -1000M$, $R_2 = 1000M$. In both cases $\mu M = 0.3$, $\ell = 1$ and $v = 0$. The spectra are shown in Fig. 3.

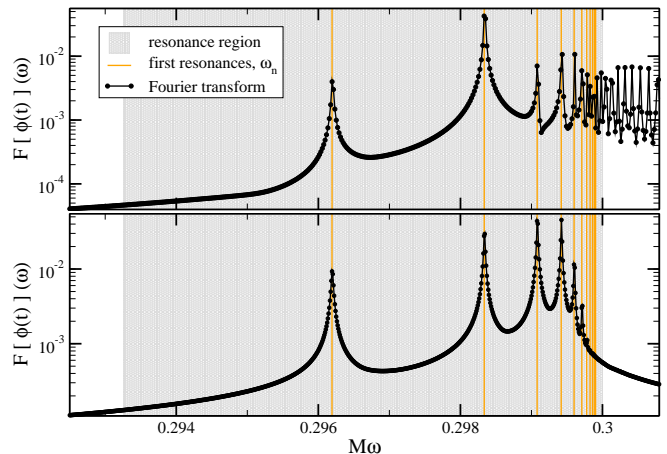


FIG. 3: Fourier transform in time of the evolution of initial data with $R_1 = 100$, $R_2 = 200$ (top panel); and $R_1 = -1000$, $R_2 = 1000$ (bottom panel). The peaks to the right of the resonance band in the top panel are a numerical artifact caused by noise originating at the outer boundary.

For comparison, we have indicated in the figure the first resonance frequencies (vertical lines), as obtained in [3]. One can clearly see peaks that coincide with each resonant frequency. These results seem to indicate that, at late times, even quite generic SF distributions evolve as a combination of the resonant modes, which, as we have shown, can last for cosmological time-scales.

This work was supported in part by CONACyT grants 82787 and 167335, DGAPA-UNAM through grant IN115311, and SNI-México. JCD and MM acknowledge DGAPA-UNAM for postdoctoral grants. OS was also

supported by grant CIC 4.19 from Universidad Michoacana. This work is part of the “Instituto Avanzado de Cosmología” collaboration.

-
- [1] J. D. Bekenstein, Phys. Rev. **D51**, 6608 (1995).
- [2] I. Pena and D. Sudarsky, Class. Quant. Grav. **14**, 3131 (1997).
- [3] J. Barranco, A. Bernal, J. C. Degollado, A. Diez-Tejedor, M. Megevand, et al., Phys.Rev. **D84**, 083008 (2011), 1108.0931.
- [4] S.-J. Sin, Phys. Rev. **D50**, 3650 (1994), hep-ph/9205208.
- [5] A. Arbey, J. Lesgourgues, and P. Salati, Phys. Rev. **D64**, 123528 (2001), astro-ph/0105564.
- [6] L. A. Urena-Lopez and A. R. Liddle, Phys. Rev. **D66**, 083005 (2002), astro-ph/0207493.
- [7] A. Cruz-Osorio, F. S. Guzman, and F. D. Lora-Clavijo, JCAP **1106**, 029 (2011), 1008.0027.
- [8] P. Sikivie and Q. Yang, Phys.Rev.Lett. **103**, 111301 (2009), 0901.1106.
- [9] J. Grain and A. Barrau, Eur.Phys.J. **C53**, 641 (2008), hep-th/0701265.
- [10] A. Ohashi and M.-a. Sakagami, Class.Quant.Grav. **21**, 3973 (2004), gr-qc/0407009.
- [11] S. Detweiler, Phys. Rev. **D22**, 2323 (1980).
- [12] E. Leaver, Proc.Roy.Soc.Lond. **A402**, 285 (1985).
- [13] S. Iyer and C. M. Will, Phys.Rev. **D35**, 3621 (1987).
- [14] H.-P. Nollert, Class.Quant.Grav. **16**, R159 (1999).
- [15] K. Kokkotas and B. Schmidt, Living Rev. Rel. **3:5** (1999).
- [16] R. Konoplya and A. Zhidenko, Rev.Mod.Phys. **83**, 793 (2011), 1102.4014.
- [17] E. Berti, V. Cardoso, and A. O. Starinets, Class.Quant.Grav. **26**, 163001 (2009), 0905.2975.
- [18] R. A. Konoplya and A. V. Zhidenko, Phys. Lett. **B609**, 377 (2005), gr-qc/0411059.
- [19] W. Hu, R. Barkana, and A. Gruzinov, Phys. Rev. Lett. **85**, 1158 (2000), astro-ph/0003365.
- [20] T. Matos and L. A. Urena-Lopez, Phys. Rev. **D63**, 063506 (2001), astro-ph/0006024.
- [21] C. Boehmer and T. Harko, JCAP **0706**, 025 (2007), 0705.4158.
- [22] M. Megevand, I. Olabarrieta, and L. Lehner, Class. Quant. Grav. **24**, 3235 (2007), 0705.0644.